Ecological Engineering 54 (2013) 145–154

Contents lists available at SciVerse ScienceDirect

Ecological Engineering

journal homepage: www.elsevier.com/locate/ecoleng

Daily dynamics of radiation surface temperature of different land cover types in a temperate cultural landscape: Consequences for the local climate

Petra Hesslerová [a,*], Jan Pokorný [a], Jakub Brom [b], Alžběta Rejšková – Procházková [a]

[a] ENKI, o.p.s., Dukelská 145, Třeboň 379 01, Czech Republic
[b] Department of Landscape Management, Faculty of Agriculture, University of South Bohemia in České Budějovice, Studentská 13, České Budějovice 370 05, Czech Republic

ARTICLE INFO

Article history:
Received 8 November 2012
Received in revised form 14 January 2013
Accepted 20 January 2013
Available online 28 February 2013

Keywords:
Solar energy distribution
Water
Vegetation
Climate
Airship thermal scanning

ABSTRACT

Surface temperature (T_s) is directly related to the capacity of every ecosystem to direct energy to different heat fluxes. Vegetation with a sufficient supply of water is able to cool down the surface by enhancing the latent heat flux via evapotranspiration. We chose seven types of land covers common in a temperate agricultural landscape and used a combined method of airship thermal scanning of T_s and ground measuring of thermodynamic T_a to show their T_s and T_a (air temperature) characteristics under high solar irradiance and their consequences for local climate; simultaneously we showed that this temperature difference increases with water content. A combined method of airship thermal scanning of T_s and ground measuring of thermodynamic T_a was used. The localities differed markedly in both the values and the dynamics of T_s and $T_s - T_a$. In the early afternoon the difference in T_s between the different land covers reached almost 20 °C. Ecosystems with non-functional or no vegetation largely resembled the asphalt surface, whereas the ecosystems covered with dense, bushy or tree vegetation showed relatively well balanced daily temperature dynamics with low temperature extremes and a slow temperature morning increase or afternoon decrease. $T_s - T_a$ at the peaking solar irradiance ranged between −1 °C at the forest and 14–17 °C at the dry harvested meadow and the asphalt surface respectively. We highlight the importance of T_s as a measurable indicator of ecosystem and landscape functioning and outline the importance of functional vegetation for climate. Those feedbacks between vegetation, surface temperature, water and climate are crucial in the landscape management, climate change discussions and therefore for decision makers and landscape developers.

1. Introduction

Under appropriate conditions vegetation is able to transfer – via evapotranspiration – a major part of incoming solar radiation (several hundreds of watts m^{-2}) into latent heat of water through phase transition (Penman, 1948). Consequently, it plays an essential role in energy dissipation and landscape energy balance and thus impacts the Earth's surface temperature as well as chemical and biological processes in ecosystems (Eiseltová et al., 2012; Ripl, 2003; Kadlec, 2009). Man controls the distribution of incoming solar energy by management of water and vegetation. During hot sunny in temperate zone, daily income of solar energy is about 7 kWh m^{-2}/day, with a maximum of solar irradiance 800–1000 W m^{-2}. The way how this energy is distributed depends on water availability and type of land cover. Sealed dry surface converts the majority of it into sensible heat, responsible for landscape heating; on the contrary functional vegetation, supplied with water (as forest, wetlands are) dissipates this energy harmlessly through water evapotranspiration, which means conversion into latent heat, responsible for landscape cooling. The indicator that reflects how the solar energy is dissipated is surface temperature. Destruction of functional ecosystems by inappropriate landscape management leads to a surface temperature increase and consequences on regional climate (low air humidity in summer, temperature fluctuation, and unevenly distributed rainfall). Large temperature differences in the landscape increase gradients that can be manifested by higher air flow/wind speed and landscape drying. Mineralization processes and erosion are accelerated; matter and nutrient losses exhaust the landscape (Ripl, 2003; Pokorný, 2001).

Nevertheless, in sustainable development strategies and climate change science, these changes in vegetation/land cover are being considered mainly in relation to changes of surface reflectivity (IPCC, 2007; Bala et al., 2007; Bonan, 2008; Trenberth, 2004)

* Corresponding author. Tel.: +420 384 706 173; fax: +420 384 724 346.
E-mail addresses: hesslerova@enki.cz (P. Hesslerová), pokorny@enki.cz (J. Pokorný), jbrom@zf.jcu.cz (J. Brom), berejska@gmail.com (A. Rejšková – Procházková).

0925-8574/$ – see front matter © 2013 Elsevier B.V. All rights reserved.
http://dx.doi.org/10.1016/j.ecoleng.2013.01.036

and sink/source shifts of carbon dioxide (IPCC, 2007; Strassburg et al., 2009; Liski et al., 2000). Yet Cook et al. (2011) considered anomalous sea surface temperatures, together with land cover change as main causes of the period of drought in North America between1932 and 1939 – the "Dust Bowl".

Changes of temperature can be observed by measuring standard air temperature (T_a, thermodynamic temperature) or by measuring or scanning surface temperature (T_s, radiative surface temperature; for terminology see Norman and Becker (1995)). T_a is usually measured in a screen (2 m above the ground) by a standardized method, the purpose of which is to minimize the effect of surface characteristics on the measured T_a. T_s is usually measured by systems detecting radiation reflected or emitted in the thermal part of the electromagnetic spectrum (commonly in 7–14 μm). Large scale scans can be provided either by satellites (e.g. Landsat, Terra Aster and MODIS, NOAA-AVHRR) or airplanes. Even though T_s represents an important source of input data for climate, evaporation and temperature modelling (Quattrochi and Luvall, 1999, 2004), the ambiguous terminology often results in mistaking T_s for near-surface air temperature and vice versa (such as in Dang et al., 2007).

T_a is often interpolated to larger areas and presented as the surface temperature of the landscape even though it is often very different from T_s (Lillesand and Kiefer, 2000; Katsiabani et al., 2009).

The relation between surface temperature and vegetation density (in the form of Normalized Difference Vegetation Index – NDVI), patterns and dynamics has been used in a number of applications, (e.g. Lambin and Ehrlich, 1996; Hesslerová and Pokorný, 2010a; Nemani and Running, 1997; Brom et al., 2012). However, the correlation between these two variables changes with whichever factor is limiting vegetation growth at the time, such as energy, air temperature or water (Karnieli et al., 2010). It is therefore essential to study the relation between surface temperature and land cover characteristics empirically and site-specifically. Until now, published articles have focused only on surface temperature characteristics of homogenous, large scale agricultural areas (Xiao and Weng, 2007; Jiang and Tian, 2010; Le-Xiang et al., 2006; Melesse, 2004; Carlson and Arthur, 2000; Lambin and Ehrlich, 1997; Saunders et al., 1998) and their relation to the water regime, gains, soil or evapotranspiration characteristics of the crops at the time (Moran et al., 1994; Riecosky et al., 1994; Mihailovic and Eitzinger, 2007; Wanjura et al., 2004). Changes in surface temperature have been studied also in relation to the impact of vegetation expanses in urban areas (Quattrochi and Ridd, 1998; Jenerette et al., 2007; Li et al., 2012) and as a cooling effect of green roofs on indoor temperatures (Jim and He, 2010; Teemusk and Mander, 2010).

T_s indicates the way solar radiation is transformed at the Earth surface. Even though the tight relation between landscape management (especially changes in land use and land cover) and climate has been discussed in the literature (Pielke et al., 2006; Foley et al., 2003, 2005; Davey et al., 2006; Ryszkowski and Kędziora, 2008; Yokohari et al., 1997), detailed studies on T_s temporal and space dynamics of various types of land covers such as fields, meadows, forests, wetlands, small water surfaces within one area of similar climatic conditions and solar exposition are lacking. There are only few studies considering daily or seasonal dynamics of T_s (Herb et al., 2008; Katsiabani et al., 2009). Leuzinger et al. (2010) measured T_s of ten common tree species in urban area and compared it with T_a in terms of their cooling effect during hot periods. Studies of this sort have usually focused on changes in land cover related to changes in atmospheric temperature (Kalnay and Cai, 2003; Nuñez et al., 2008) or modelled atmospheric temperature (Dang et al., 2007) only. The temperature dynamics of T_s as a reflection of water stress has so far been used for field irrigation optimization (Peters and Evett, 2007; Mihailovic and Eitzinger, 2007; Wanjura et al., 2004). An ecosystem temperature could be perceived as an indicator of the "ecosystem health" as a body temperature is – low or high is not good (Costanza, 2012).

This paper loosely extends the study Hesslerová et al. (2012) combining satellite surface temperature and water hydrochemistry parameters in six catchments, different in land cover. Here, we use a combined method of airship scanning of T_s and ground measuring of T_a in a varied agricultural landscape, to show the daily dynamics of T_s and T_a at localities with different land cover. The aims of our study were

1. to record and quantify the differences in spatial and temporal dynamics of T_s during a hot summer day within a cultural landscape of high land cover variability (forest–wet meadow–field–asphalt)
2. to compare daily dynamics of the surface temperature T_s of the studied localities with air temperature T_a
3. to discuss and point out how landscape planners and engineers may affect local climate by dealing with water and vegetation

2. Materials and methods

2.1. Site description

The area studied is located in the centre of the rather flat (410–470 m a.s.l. ascending up to 550 m a.s.l. to the margins) Třeboň Basin Biosphere Reserve near the town of Třeboň, South Bohemia, the Czech Republic (49°05′N, 14°46′E, 428 m a.s.l.). Originally a peaty marsh, the Reserve is nowadays dominated by man-made lakes. Its extraordinary high diversity of habitats and species has led to its designation as a Ramsar Site of International Importance and a UNESCO Man and Biosphere Programme (Květ et al., 2002). For many years this area has been used also for ground measurement of water and energy fluxes in different ecosystems (Huryna and Pokorný, 2010; Rejšková et al., 2012; Pokorný et al., 2010a), and for relating the remote sensed surface temperature to vegetation density and water supply (Hesslerová and Pokorný, 2010a).

Seven localities with different land cover types were chosen, southeast of the village of Domanín (about 5 km southeast of the town of Třeboň) (Fig. 1).

Locality 1 (HM) – harvested mesic meadow covered with drying out grass of about 10 cm length. Dominant species were *Alopecurus pratensis* L. and *Arrhenatherum elatius* (L.) J. Presl & C. Presl.
Locality 2 (WM) – wet meadow with high underground water level, dominant species: *Phalaris arundinacea* L. and *Carex* sp., cover height of approx. 1 m.
Locality 3 (AS) – alder stand, floodplain community of *Alnus glutinosa* L. and *Prunus avium* L., shrubs and smaller trees of up to 3 metres high.
Locality 4 (F) – mixed forest represented mainly by pine trees (*Pinus sylvestris L.*) and oaks (*Quercus robur* L.); estimated age 60 years, average cover height 10–15 m.
Locality 5 (SV) – bare field (loamy-clay soil), less than 50% of the area covered by sparse grass vegetation.
Locality 6 (W) – open surface water. Shallow pond with maximum depth of 1.5 m and intensive fish farming.
Locality 7 (A) – asphalt surface of a road.

2.2. Remote sensing measurement of surface temperature T_s

The measurements were carried out on July 9th 2010. The thermographic cameras as well as the visible camera were carried by an airship. The thermographic camera IR FPA ThermaCAM™ PM695

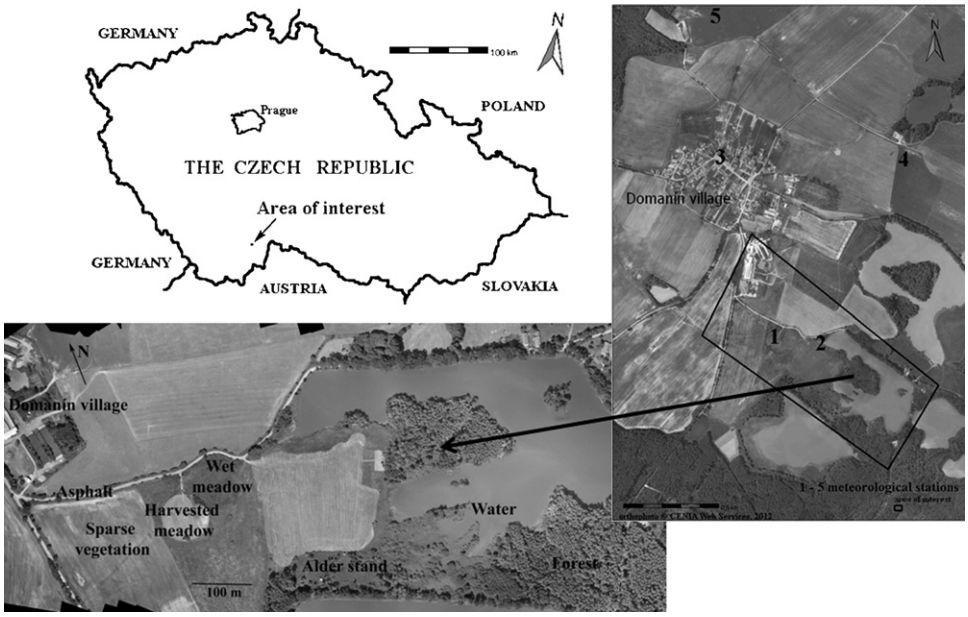

Fig. 1. A detailed picture of the area under review with the depicted studied localities and its localization on a map of the Czech Republic.

(Flir System Sweden) measures and images infrared (IR) radiation emitted from an object in the spectral range from 7.5 μm to 13 μm with the spatial resolution of 320 × 240 pixels (pixel size of 30 cm) and thermal sensitivity of 0.08 °C at 30 °C. The radiation detected by the camera is influenced by objects' emissivity, reflected radiation from the surroundings and atmospheric absorption of radiation. The precise temperature measurement is subject to accurate compensation of different sources of radiation. The calibration requires the following parameters: object's emissivity, reflected surrounding temperature, distance between the object and camera, relative humidity and atmospheric temperature. The calibration parameters were obtained from the screens situated within the area of interest; the emissivity parameters as standard table values.

The nine-metre long airship (AirshipClub.com) was equipped with an advanced navigation and control systems that allowed it to fly in an automatic mode along a precisely defined route navigated by GPS (for details see Jirka et al., 2011). It flew about 250 m above the ground, the swath being about 200 m. In order to monitor the surface temperature throughout the light part of a sunny day, the area was scanned 16 times (at 04:50, 05:30, 06:00, 07:10, 08:10, 09:10, 10:40, 13:15, 14:00, 15:10, 16:10, 17:10, 18:10, 18:40, 19:10, 20:10 GMT+1).

2.3. Data processing

To show the temperature dynamics and to compare the selected localities, the surface temperature data were exported to a table. To reduce the huge data files while maintaining all characteristics of the original data, we applied a random data selection. A random permutation of the elements of 'x' (or '1: x') was used (for more details see Ripley, 1987). As a representative sample, 1000 values (pixels) for every locality and time were chosen. Box plots were used in the figure depicting the course of the surface temperature.

The distribution of temperature within the localities studied was compared by a variance analysis. Taking time dependency of the data into account, we used the nested design of analysis of variance (ANOVA). The locality was taken as the independent variable and time as the block. By dividing the data into groups we reduced the number of locality comparisons, thus improving the test power.

To record the daily dynamics (i.e. from 4:50 to 20:10 GMT+1), we focused on the following variables:

- Mean daily surface temperature (T_{savrg}) – mean surface temperature of a locality measured in 16 scans from 04:50 to 20:10.
- Mean surface temperature of a locality in time t (T_{st})
- Mean minimum surface temperature, mean maximum surface temperature (T_{smin}, T_{smax}) –temperature extremes recorded during the time of measurement (4:50 to 20:10 GMT+1)
- Surface temperature difference (D_s) – the difference between T_{smax} and T_{smin}
- Surface temperature fluctuation (expressed by values of standard deviation) – shows the variability of temperature at a locality at a certain time (surface temperature heterogeneity of a locality SD_{st}) or throughout the day (mean daily variability SD_{sd})

2.4. Meteorological data

We compared T_s of the studied localities with the mean air temperature measured at 2 m above the ground in meteorological screens (T_a). T_a was calculated as a mean value of data from 5 meteorological stations (Fig. 2) situated at the studied localities or nearby (Fig. 1). Due to minor differences between individual T_a values, we used this average temperature as a reference. The air temperature T_a was recorded at 10-min intervals in five meteorological screens set on the studied localities or within 1 km distance from them (Fig. 1):

Screen 1: harvested meadow – placed at locality 1 (HM)
Screen 2: wet meadow – placed at locality 2 (WM)
Screen 3: square in village covered with asphalt surface (asphalt)
Screen 4: pasture moderately grazed; community dominated by *Lolium perenne* L. (pasture)
Screen 5: winter wheat field in a milk-grain stage (field)

Air temperature was measured at 2 m above the soil surface (T_a, °C, T+Rh probes, accuracy ±0.1 °C). The course of daily air temperature was expressed as an average of 5 stations measurement (Fig. 2).

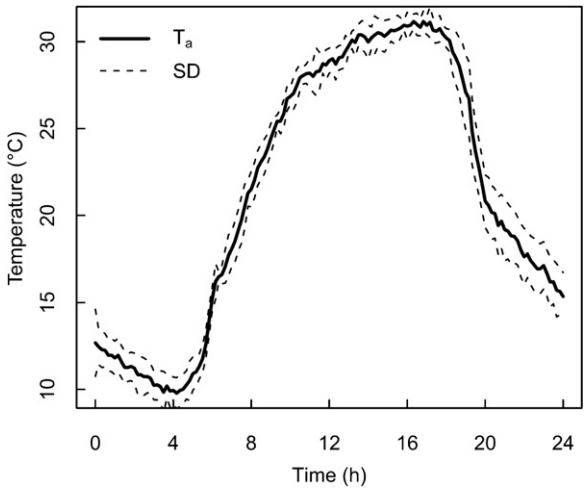

Fig. 2. Mean T_a calculated as an average value from 5 meteorological stations in the studied area.

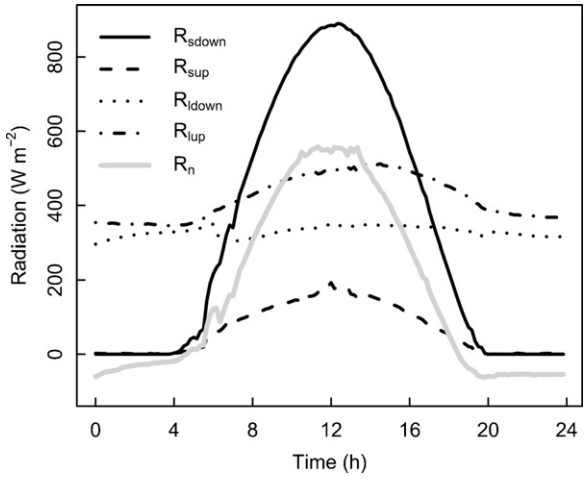

Fig. 3. Incoming shortwave ($R_{s\,down}$) and longwave ($R_{l\,down}$) radiation, reflected shortwave radiation ($R_{s\,up}$), longwave radiation emitted from the surface ($R_{l\,up}$) and net radiation (R_n) measured at the locality HM (harvested meadow) on 9 July 2010.

Variability of meteorological data is expressed in Table 3 as the standard deviation. The locality "harvested meadow" was equipped also with CNR1 net radiometer (Kipp & Zonen) for radiation balance analysis of solar and far infrared radiation (in $W\,m^{-2}$). Incident (R_{sdown}) and reflected global solar radiation (R_{sup}) in shortwave region was measured by CM3 pyranometer (Kipp & Zonen, spectral range from 0.31 to 2.8 μm), far infrared radiation (5–50 μm) was measured by two CG3 pyrgeometers, one for measuring radiation coming from the sky (R_{ldown}), the other for measuring radiation coming from the soil surface (R_{lup}). Calculation of net radiation (R_n) was based on values gained by the above mentioned instruments, using the following formula:

$$R_n = (R_{sdown} + R_{ldown}) - (R_{sup} + R_{lup})$$

3. Results

The measurements were carried out under clear sky on a hot summer day; maximum incoming solar energy was of $890\,W\,m^{-2}$. Incoming solar radiation during the day of measurement and the components of radiation balance are shown in Fig. 3.

Table 1
Mean surface temperature (T_s) characteristics of the studied localities measured by the thermal camera from 4:50 to 20:10 in sixteen scanning times. T_{smin}, temperature minimum, T_{smax}, temperature maximum, D_s, temperature difference, T_{savrg}, mean temperature, and SD_{sd}, surface temperature variability throughout the day.

Locality	T_{smin}	T_{smax}	D_s	T_{savrg}	SD_{sd}
HM	9.3	44.2	34.8	28.0	10.98
WM	10.0	31.9	21.9	22.6	6.78
AS	10.1	28.9	18.8	21.7	5.95
F	12.0	29.0	17.0	22.8	5.77
SV	13.2	37.2	24.0	26.4	7.70
W	20.4	29.3	8.9	25.6	3.41
A	16.1	47.6	31.4	33.0	10.19

HM: harvested meadow; WM: wet meadow; AS: alder stand; F: forest; SV: sparse vegetation; W: water; A: asphalt.

3.1. Surface temperature characteristics of localities with different land cover

In general, surface temperature (T_s) rose with increasing input of solar energy throughout the morning and early afternoon reaching maximum at 13:15 and decreasing again to night and early morning minimums. T_s increase was strongly related to the increasing amount of solar energy. The localities differed substantially in the mean minimum and maximum values of T_s and consequently in the daily T_s amplitudes (Table 1). However, they also differed in the T_s dynamics, especially in the afternoon decrease of temperature as follows from the site specific T_s description hereafter (Fig. 4).

3.2. T_s dynamics at the localities studied

The harvested meadow (locality 1 – HM) was characterized by high D_s of 35 °C and T_{savrg} of 28 °C. T_s variability within this area was very high especially from 10:40 to 13:15 (maximum values of SD_{st} were 2.35–2.67) and SD_{sd} of 10.98 represented the highest value from all measured land cover types. T_s instability of this locality was reflected also in high T_{savrg} of 28 °C and in the rapid morning increase and afternoon decrease of T_s of 3–5 °C/h and extreme afternoon T_s reaching up to 50 °C.

The wet meadow (locality 2 – WM) with its T_{savrg} of 22.6 °C, D_a of 21.9 °C and SD_{sd} of 6.78 showed a much more balanced T_s dynamics than HM. The afternoon T_{smax} reached up to 32.0 °C. SD_t was low, increasing slightly only in the early afternoon hours (at 14:00 is 1.65). The temperature decrease in the afternoon and early evening (13:15 to 19:10) was slower than on HM ranging values of 1.5–3 °C/h in the morning and 2–5.5 °C/h in the afternoon.

The alder stand (locality 3 – AS), an ecosystem of rather high species diversity and vertically structured in a herbaceous, a shrub and a tree layer, showed a T_s well-balanced (SD_{sd} = 5.95). With T_{smin} of 10.1 °C and T_{smax} of 28.9 °C the D_s reached only 18.8 °C. T_{savrg} was 21.7 °C. The rather high SD_{st} in the late afternoon (at 18:40 is 2.2) was caused by the differences in T_s (up to 6 °C) of the bush and the grass communities.

The forest (locality 4 – F) with its D_s of 17 °C (T_{smin} of 12.0 °C, T_{smax} of 29.0 °C) and T_{savrg} of 22.8 °C showed the best balanced T_s of all the vegetated localities studied. The morning T_s increase and especially the afternoon T_s decrease were slow (3 °C/h and less than 1 °C/h, respectively). The T_s balance of the locality was characterized by low values of SD_{st} ranging from 0.35 to 1.35.

The bare field with sparse vegetation (locality 5 – SV) showed low T_s balance characterized by high D_s of 24.0 °C and high T_{savrg} of 26.4 °C (T_{smin} = 13.2 °C, T_{smax} = 37.2 °C). T_s increase was as rapid as 6 °C/h between 9:10 and 10:40. SD_{st} was especially high in the

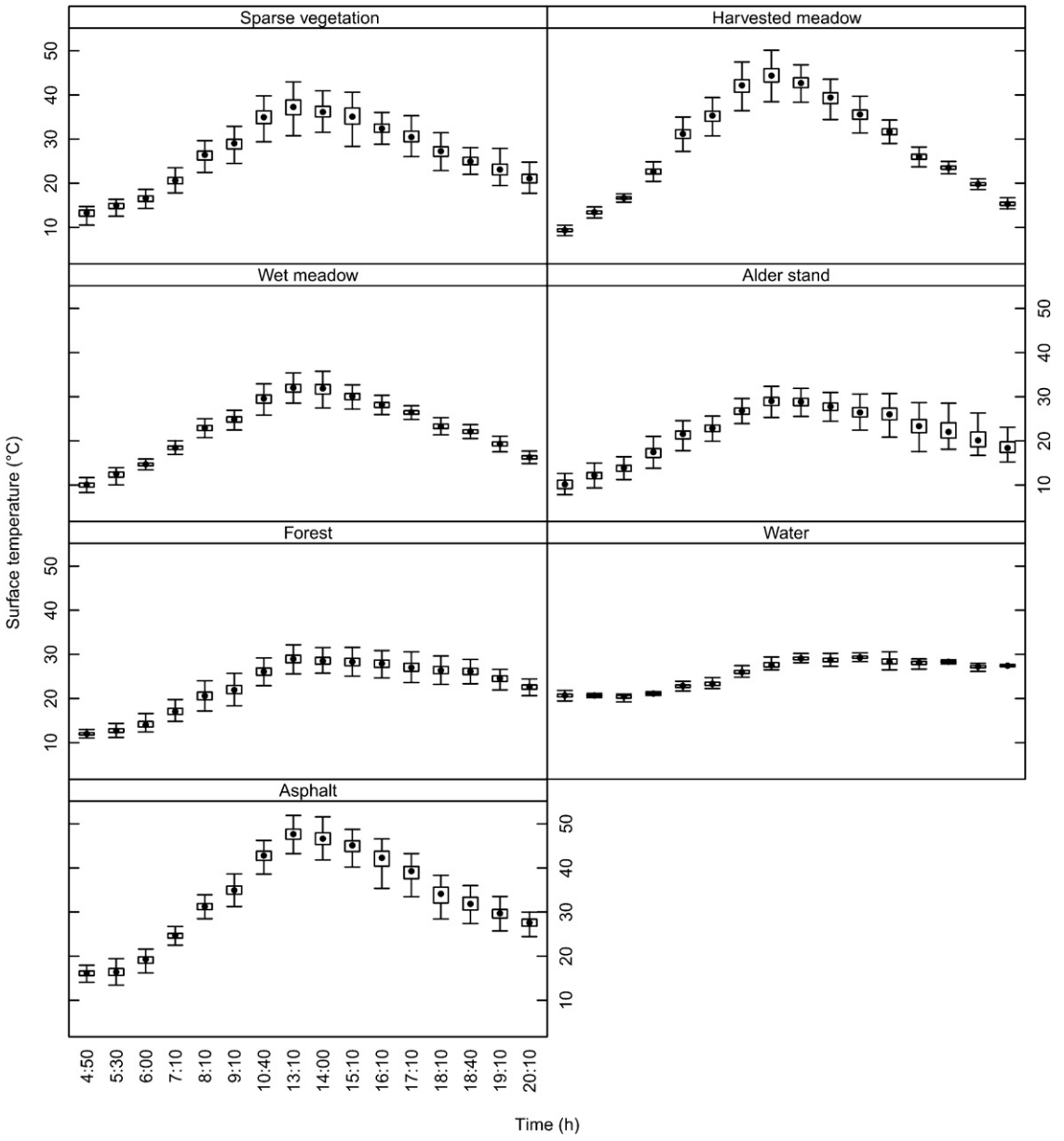

Fig. 4. Daily courses of T_s of the studied localities. Each point is calculated from 1000 randomly selected pixel values. Points describe the median of the data, boxes are lower and upper quartiles and whiskers show 1.5 times of inter-quartile range of the data or maximum and minimum values if extremes did not occur. Extreme values are not shown in the graph.

afternoon hours (2.48 at 15:10; 2.41 at 13:15), average daily T_s fluctuation (SD_{sd}) was 7.7.

The water surface (locality 6 – W) was characterized simultaneously by rather high T_{savrg} of 25.6 °C and by low D_s of only 8.9 °C and low SD_{sd} of 3.41. The T_s course was somewhat shifted if compared with T_s courses of other localities, reaching minimum values at 6:00 (20.47 °C) and maximum values at 16:10. (29.33 °C). From 17:10 on the temperature remained almost stable, oscillating between 27 and 28 °C.

The asphalt surface (locality 7 – A) was characterized by high T_{savrg} of 33.0 °C and especially by an extremely high D_s of 31.5 °C (T_{smin} = 16.1 °C, T_{smax} = 47.6 °C). The T_s increase in the morning was high (reaching 6.6 °C between 7:10 and 8:10, and as much as 8 °C between 9:10 and 10:40), the T_s decrease in the afternoon (15:10 to 19:10) was slightly slower (3–5 °C/h). The SD_{sd} of 10.19 was very high.

3.3. Comparison of surface temperature (T_s) dynamics at the studied localities

The T_s dynamics of the localities studied (Fig. 4) differed to a large extent, especially as the intensity of the incoming energy increased. In the very morning (04:50 and 05:30 takes) the differences in T_s between the localities were small. The highest T_s was that of the water surface (20.4 °C). The second warmest land cover was the asphalt surface (16.1 °C) followed by the sparsely vegetated field (13.2 °C) and the forest (12 °C). The coolest localities were the alder stand (10.1 °C) and wet (10 °C) and harvested (9.3 °C) meadows. With the increasing solar irradiance, T_s rose at all localities. The increase was slower at the localities covered with dense green vegetation (AS, F, WM). Until 06:00 the water surface had the highest T_s then it was overtaken by rapidly increasing T_s of the localities covered by sparse or dried vegetation or asphalt at

which T_s exceeded 30 °C as soon as at 8:10. The role of green vegetation was evidenced from a comparison of WM and HM, where difference increased from early morning. At noon T_s of HM was already 12.2 °C higher than T_s of WM.

The largest inter-localities variability was reached during the peak of solar irradiance input (10:40 to 15:10). Coolest localities were those with high and dense vegetation (excluding W) i.e. AS and F. T_{smax} of these localities did not exceed 29.0 °C. T_{max} of WM covered with grassy vegetation reached values of about 3 °C higher than in case of AS and F. T_s of the remaining three localities with dry to no vegetation, i.e. HM, SV and A, rose to extreme values. In the morning T_s at SV still remained around 30 °C, however during the afternoon extreme solar irradiance (13:10) it reached the mean maximum of 37.2 °C. Mean T_s at HM and A climbed up to 42 °C already at 10:40. T_{max} equalled 44.2 °C and 47.6 °C at 13:10 at HM and A respectively.

In the late afternoon (16:10 to 18:10) the localities of extreme T_s cooled down gradually and the differences between their T_s became smaller. The rate of cooling differed at different localities. Whereas at 16:10 F and W together with AS and WM were the coolest localities, by 18:10, due to their slow cooling rates (about 2.2 °C/h between 18:10 and 20:10), F and W remained among the warmest localities. A more pronounced decrease of temperature was recorded at HM (4 °C/h between 17:10 and 18:10, a hour later it was even 6 °C/h). A rapid temperature decrease of 4 °C between 18:40 and 19:10 was measured also at A; however this locality remained very hot until the last scanning (27.6 °C at 20:10).

The localities differed significantly among themselves, when compared during the day and in individual scanning times with ANOVA with Tukey HSD post hoc test (Table 2).

Our analysis showed that all the localities are significantly different ($p < 0.001$ in all cases). Comparison at a particular time showed significant differences in most cases. Twelve comparisons showed no statistically significant difference, mostly in morning and evening hours.

3.4. Comparison of surface temperature T_s and air temperature T_a

During highest irradiance (13:10), the maximum difference of T_a (difference between the maximum and minimum temperature measured in this time in the screens) was 1.3 °C. Somewhat larger differences were observed only before the sunset when large changes in radiation balance occurred. The extreme values were measured between the screens in wet meadows and asphalt (at 19:10 6 °C). The differences between T_s and T_a grew with the increasing amount of incoming solar radiation and varied substantially depending on the type of the land cover (Fig. 5 and Table 3). After sunrise, T_s at AS and F, the localities with dense vegetation and sufficient supply of water, was lower than T_a and the difference grew in the late afternoon to as much as 6.7 °C at 18:10 at AS. T_s of WM oscillated around T_a with T_s exceeding T_a by no more than 2 °C at the time of the highest intensity of solar insolation. After 15:10 T_s at WM decreased more rapidly than T_a and the differences became more pronounced. T_s of SV and HM, the localities with dry or sparse vegetation, exceeded T_a during the peaking solar irradiance by as much as 7 °C and 14 °C respectively. On the other hand T_s was lower than T_a at SV and HM during the evening hours as was mostly the case at all vegetated surfaces. T_s of the asphalt surface was higher than T_a during the whole day. The difference reached the maximum of as much as 17.5 °C during the early afternoon hours of maximum solar energy input. T_s of the water surface was higher than T_a especially in the morning and in the evening. During the day T_s of W was slightly lower than T_a.

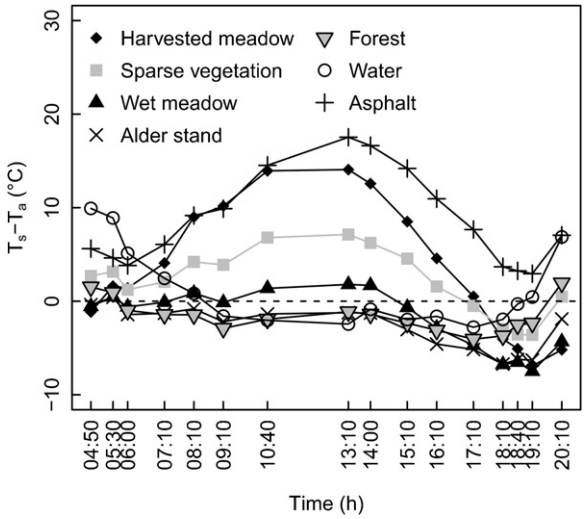

Fig. 5. Temperature differences $T_s - T_a$ between surface T_s and air temperature T_a (at 2 m above ground) at all studied localities.

4. Discussion

4.1. T_s at sites with different land cover

T_s and its daily dynamics of the studied localities with different types of land cover were significantly different during a hot sunny day. The most distinct differences were found between the localities with dry or sparse vegetation and those with fully functional vegetation and sufficient water supply (Table 1). T_s characteristics of the ecosystems with non-functional or no vegetation largely resembled the asphalt surface (T_{smax} 47.6 °C, D_s 31.4 °C), whereas those with dense vegetation were influenced by the presence and phase transition of water (water surface: T_{smax} 29 °C and D_s only 9 °C due to high heat capacity of water). The localities covered with dense bushy or tree vegetation showed relatively well-balanced daily T_s dynamics (Fig. 4) with low T_s extremes and a slow morning increase or afternoon decrease of T_s. The impact of vegetation and water presence on the ecosystem's T_s dynamics was clearly demonstrated on the wet meadow locality which showed much more balanced T_s compared to the nearby situated harvested meadow covered with dry vegetation.

Plants via evapotranspiration provide the living systems with a highly effective thermoregulative mechanism (2.5 MJ/kg^{-1} at 20 °C are spent during evaporation and released during condensation of water). The cooling and warming effects of water liquid-gas transition can be multiplied within the vegetation, especially within high forest stands, thank to higher temperature and structural variability (see Makarieva et al., 2006; Eiseltová et al., 2012; Pokorný et al., 2010a; Hesslerová and Pokorný, 2010b; Kędziora, 2010). Teuling et al. (2010) analyzed and compared role of forest and grassland during heatwave days in Europe in terms of solar energy exchange, with a result of highlighting the dual role of forest which means accommodation of sensible heat and storage of water for survival.

4.2. Comparison of T_s and T_a of different land covers

The air temperature T_a measured in a screen 2 m above the ground is accepted as the standardized air temperature and its characteristics are used as an indicator of climate and climate change (IPCC, 2007). The T_a measured in the 5 meteorological screens within the studied area (Fig. 1) did not differ much during the insolated part of the day (Table 3). During the midday, the

Table 2
Results of an analysis of variance (ANOVA) – the localities were compared between and among themselves and in individual scanning times. d.f.: degrees of freedom; Sum Sq.: sum of squares; mean Sq.: mean square; *F*: *F* value of testing criteria; *p*: probability value.

Factors	d.f.	Sum Sq.	Mean Sq.	*F*	*p*
Locality	6	1,488,786	248,131	135,222	<0.001
Locality:Time	105	6,353,166	60,506	32,974	<0.001
Residuals	111,888	205,314	2		

Table 3
Comparison of mean T_a and T_s of the studied localities during the day of measurement. SD_a: standard deviation of air temperature.

Time	Mean T_a at 2 m [°C]	SD_a	Mean surface temperature (T_s) of the localities (remote sensing) [°C]						
			Harvested meadow	Wet meadow	Alder stand	Forest	Sparse vegetation	Water	Asphalt
4:50	10.5	1.13	9.3	10.0	10.1	12.0	13.2	20.4	16.1
5:30	11.8	0.81	13.4	12.2	12.9	12.7	14.9	20.7	16.4
6:00	15.2	0.68	16.7	14.6	13.8	14.3	16.5	20.4	19.1
7:10	18.5	1.16	22.6	18.4	17.2	17.1	20.6	21.0	24.7
8:10	22.0	1.02	31.0	23.0	21.2	20.6	26.2	22.9	31.2
9:10	25.0	0.71	35.1	25.0	22.8	22.0	28.8	23.4	34.8
10:40	28.0	0.49	42.0	29.4	26.7	26.1	34.9	26.0	42.6
13:10	30.1	0.51	44.2	31.9	28.9	29.0	37.2	27.7	47.6
14:00	30.0	0.97	42.6	31.7	28.7	28.6	36.2	29.1	46.6
15:10	30.7	0.64	39.9	30.0	27.6	28.3	35.2	28.7	44.9
16:10	31.0	0.52	35.5	28.9	26.4	27.9	32.5	29.3	41.9
17:10	31.1	0.88	31.6	26.4	26.0	27.1	30.6	28.3	38.8
18:10	30.1	0.64	26.0	23.3	23.4	26.4	27.1	28.1	33.8
18:40	28.6	1.62	23.5	22.1	22.4	26.1	25.0	28.3	31.9
19:10	26.7	2.11	19.8	19.2	20.4	24.4	23.1	27.2	29.7
20:10	20.6	1.62	15.4	16.2	18.7	22.5	21.1	27.4	27.6

differences between the screens ranged around 1 °C or even less; the maximum difference was measured before sunset (19:10 and 20:10), when it reached 6 °C (between asphalt and wet meadow screens) and 4.6 °C (asphalt and field). Huryna and Pokorný (2010) analyzed in the same area the air temperature at six different sites – fishpond, wet meadow, pasture, barley field, village and concrete surface in 183 days of the vegetative season. In addition the season was divided into three classes according to the amount of incoming solar energy they received. The seasonal analyses confirmed little air temperature differences. The daily average air temperature difference between the sites on the overcast days was 1.05 °C, on clear days was 2.1 °C and 1.6 °C on cloudy days. Whereas T_a was relatively similar at different places of the studied area (Table 3), the maximum difference of T_s between the different studied land covers reached almost 20 °C in the early afternoon (Table 3 and Fig. 4). The substantial difference in $T_s - T_a$ at localities with different land cover, both in values and the characteristics of the daily courses imply that it is essential to consider the relations between T_s and T_a site specifically.

In general, high irradiation causes surface temperature to be higher than air temperature 2 m above the surface (Pal Arya, 2001; Katsiabani et al., 2009; Gallo et al., 2011). However $T_s - T_a$ strongly varies according to the land cover type and can reach even negative values. Also the daily courses of these variables differ. Whereas the surface temperature peaks around 12:30 simultaneously with the maximum intensity of irradiance, the air temperature peaks later in the afternoon between 16:00 and 17:00 (Table 3; Fig. 4). Large differences in $T_s - T_a$ of almost 15 °C at the maximum of incoming irradiance (Table 3) were found at the localities with sparse or dry vegetation. At the same time T_s of the localities covered with dense vegetation well supplied with water (wet meadow, alder stand and forest) was even slightly lower than T_a. Even though the comparison of T_s and T_a could have been influenced by the different height of the compared stands (air temperature was measured 2 m above the meadow whereas the forest was 10–15 m tall), the temperature differences were large enough to express the influence of functional vegetation on T_s increase. Moreover, taking into account the fact that T_a commonly changes in adiabatic lapse rate of 0.6 to 1 °C/100 m of elevation, the differences of T_a above a meadow and an adjacent forest stand should not be large.

The difference of T_s and T_a is usually mentioned in meteorological and climatological textbooks; however, the consequences resulting from this difference do not frequently appear in climate change discussions, recommendation and what is the most important – are not applied in climate change mitigation strategies. The large differences between both temperatures and between the sites with high temperature differences cause high temperature gradients – the consequence is higher turbulent heat flux, higher wind speeds and drainage of the landscape. A landscape without water converts the majority of incoming solar radiation into sensible heat, that it responsible for its heating. Our results show that water and its presence in the landscape – not only in the form of water bodies, but mainly its content in vegetation and soil, is able to balance temperature differences, keep surface temperature lower and therefore not lose water.

4.3. Different surface temperature and ecosystem functioning

There has been several years experience in thermal analyses of the landscape (Huryna and Pokorný, 2010; Pokorný et al., 2010a,b; Procházka et al., 2011; Rejšková et al., 2012; Brom and Pokorný, 2009; Jirka et al., 2009), involving meteorological measurements, thermal analysis of different ecosystems – radiation and energy balance in several seasonal time series and thermal data calibration. Vegetation is very heterogeneous when it comes to solar energy distribution; therefore it is inappropriate to approximate the thermal response of different land cover types by seasonal averages – the extremes are important – especially when it comes to climate change. Enhancing the role of vegetation in extreme conditions – during hot sunny days – could play a role in mitigating climate change.

The cultural landscape of this study represents a highly heterogeneous mosaic of T_s. During maximum solar irradiance the difference of T_s between the studied localities was as high as 19.9 °C.

The localities with maximum T_s were also characterized by high vertical temperature gradients ($T_s - T_a$). The difference between T_s and T_a was 15 °C and 20 °C (temperature gradient for 2 m) at the harvested meadow and the asphalt surface respectively.

Large vertical and horizontal temperature gradients result in air thermal turbulence (Pal Arya, 2001). Differential heating caused by sensible heat gradients across adjacent regions of intensively transpiring vegetation and dry, bare soil can even generate a sea breeze-like circulation, called a "vegetation breeze" (Eltahir and Bras, 1996; Pielke, 2001; McPherson, 2007). Regional and large scale land cover/use changes may modify local climatic conditions more than climate change itself (e.g. Shaver et al., 2000; Lawton et al., 2001; McPherson, 2007). Thermal turbulence supports evaporation of water and its loss from the area in terms of donor and acceptor zones defined by Makarieva and Gorshkov (2010). Under diminishing water supply, the surface temperature of drying areas rises even further. Such overheated areas are prone to excessive decomposition of organic material, loss of nutrients and erosion (Ripl, 2003) with definite negative consequences for landscape functioning (Hesslerová et al., 2012).

The variability of the surface temperature is natural, related to the water supply conditions, soil and topographic characteristics as well as ecosystem composition. However, the decline of functional vegetation due to vast land cover changes in the cultural landscape of Europe has led to an enormous shift to large surfaces which have high surface temperature during high irradiance. The sensible heat flux from the built up areas of the Czech Republic (an area of about 2586 km^2, Miko and Hošek, 2009) equals about 3.6 MWh on one sunny day. Agriculture has also extensively changed the temperature conditions of the Earth's surface. Most of our common crops are to a large extent xerophytic and require fields with low water level, green for only a short period of the year. In the summer such fields are often already covered with dry ripening vegetation with T_s characteristics similar to the studied harvested meadow. Moreover, for long periods of time the fields are bare with no vegetation. During this period and under high solar irradiance their T_s resemble the high irradiance temperatures of opencast mines (Hesslerová and Pokorný, 2010a).

Solar energy comes to the Earth surface in daily pulses depending on the weather, season and geographical position. Highly developed natural biological systems are able to dissipate the excessive solar energy so that T_s extremes are avoided (Eiseltová et al., 2012). This is very important for landscape functioning, especially from the long-term point of view as temperature extremes contribute to landscape ageing.

4.4. Land cover and environmental policy

The relation between vegetation and T_s is common knowledge – everybody knows that on a hot sunny day the air is cooler in a forest than on a bare field. It is the surface temperature that living organisms are in contact, and the microclimate that is created within ecosystems, that is crucial for the functioning of biological systems. Our results show that under high irradiance the differences in T_s are extreme even within a highly varied agricultural landscape.

Intensification of agriculture and urbanization has a significant share in disruption of energy flows. Due to landscape drainage, removal of functional and permanent vegetation (not only deforestation but also the loss of hedgerows, scattered vegetation, wetlands, wet meadows and preferences of thermophilous crops), leads to overheating of the landscape and its degradation; this may be demonstrated by rapid removals of nutrients. The surface temperature of agriculture landscape during late ripening and above all after crops harvesting, has the same values as the industrial and mining landscape (Hesslerová and Pokorný, 2010a). Therefore land managers (owners, farmers, foresters, fishermen) should be considered as significant controllers of the solar energy distribution, i.e. "local climate constructors" namely through reasonable water and vegetation management.

All the climate models are based on the correlation of CO_2 and air temperature, but we may consider it as an unproven causal relationship. The standardized measurements of air temperature are thus deliberately set up to eliminate any differences that may be caused by the surface. Carbon dioxide is considered as a main greenhouse gas – despite being significantly more efficient in capturing thermal photons than water vapour, its concentration in the atmosphere is nearly negligible when compared to water and water vapour. Climate change literature refers to radiative forcing in the order of single (1–3) W m^{-2}, yet the release of several hundreds of watts in the form of sensible heat from the drained and bare ground is neglected. Despite the fact that latent heat flux is associated with climate models, relevant physical effects associated with water, nor the biophysical processes in vegetation; why is this?

Few scientific papers enhance the role of vegetation/land cover in climate. In the IPCC reports that serve as a scientific background and recommendation for the climate policy makers and politicians, responsible for our environment, the importance of functional vegetation/land cover is mentioned only as "it may have some role". The recommendations of IPCC to decision makers only follow the line the correlation of CO_2 and air temperature (Ripl, 2010).

Temperature balancing measures such as water retention and introduction of permanent vegetation should be adopted in the cultural landscape to retain its sustainability. Moreover, vegetation supports not only temperature balance but also water cycling on regional to global scale by its structure and physiological functioning (Makarieva et al., 2006; Makarieva and Gorshkov, 2007, 2010; Kędziora, 2010; Foley et al., 2003, 2005; Piao et al., 2007; Pielke, 2005). These studies suggest clearly that land use/cover change must be included in global and regional strategies to effectively mitigate climate change (McAlpine et al., 2009; Kravčík et al., 2007).

5. Conclusions

During high solar irradiance, forests and vegetation well supplied with water are cooler and more temperature-balanced than areas with dry or sparse vegetation. High vertical temperature gradients between surface temperature and air temperature develop at the dry surfaces characterized by high surface temperature and large temperature fluctuations. Vegetation and water mitigate surface temperature fluctuations. Drainage, deforestation and removal of permanent vegetation cause surface temperature to rise. This is not directly reflected by standard measurements of air temperature. Surface temperature is tightly connected to the local-regional climate. Feedbacks between vegetation, surface temperature, water and climate are crucial in the landscape management, climate change discussions and therefore for decision makers and landscape developers. We have introduced a method of airship thermal scanning that may be used for landscape assessment in terms of its thermal efficiency. Our results serve as evidence that restoration of permanent vegetation (forest, wetlands) and water retention in the landscape are important instruments for sustainable landscape development and climate change mitigation being in hands of land managers.

Acknowledgements

This paper was supported by the projects of The Ministry of Education, Youth and Sports of the Czech Republic (NPV 2B06023 and CZ.1.07/2.4.00/31.0213).

References

Bala, G., Caldeira, K., Wickett, M., et al., 2007. Combined climate and carbon-cycle effects of large-scale deforestation. PNAS 104 (16), 6550–6555.

Bonan, G.B., 2008. Forests and climate change: forcings, feedbacks, and the climate benefits of forests. Science 320, 1444–1449.

Brom, J., Pokorný, J., 2009. Temperature and humidity characteristics of two willow stands, a peaty meadow and a drained pasture and their impact on landscape functioning. Boreal Environ. Res. 14, 389–403.

Brom, J., Nedbal, V., Procházka, J., et al., 2012. Changes in vegetation cover, moisture properties and surface temperature of a brown coal dump from 1984 to 2009 using satellite data analysis. Ecol. Eng. 43, 45–52.

Carlson, T.N., Arthur, S.T., 2000. The impact of land use—land cover changes due to urbanization on surface microclimate and hydrology: a satellite perspective. Global Planet. Change 25, 49–65.

Cook, B.I., Seager, R., Miller, R.L., 2011. Atmospheric circulation anomalies during two persistent North American droughts: 1932–1939 and 1948–1957. Clim. Dyn. 36, 2339–2355.

Costanza, R., 2012. Ecosystem health and ecological engineering. Ecol. Eng. 45, 24–29.

Dang, H., Gillett, N.P., Weaver, A.J., et al., 2007. Climate change detection over different land surface vegetation classes. Int. J. Climatol. 27, 211–220.

Davey, C.A., Pielke Sr., R.A., Gallo, K.P., 2006. Differences between near-surface equivalent temperature and temperature trends for the Eastern United States Equivalent temperature as an alternative measure of heat content. Global Planet. Change 54, 19–32.

Eiseltová, M., Pokorný, J., Hesslerová, P., et al., 2012. Evapotranspiration—a driving force in landscape sustainablility. In: Irmak, A. (Ed.), Evapotranspiration—Remote Sensing and Modeling. , pp. 305–328, InTech.

Eltahir, E.A.B., Bras, R.L., 1996. Precipitation recycling. Rev. Geophys. 34 (3), 367–378.

Foley, J.A., Costa, M.H., Delire, C., et al., 2003. Green surprise? How terrestrial ecosystems could affect earth's climate. Front. Ecol. Environ. 1 (1), 38–44.

Foley, A.J., DeFries, R., Asner, G.P., et al., 2005. Global consequences of land use. Science 309, 570–574.

Gallo, K., Hale, R., Tarpley, D., et al., 2011. Evaluation of the relationship between air and land surface temperature under clear- and cloudy-sky conditions. J. Appl. Meteorol. Clim. 50, 767–775.

Herb, W.R., Janke, B., Mohseni, O., et al., 2008. Ground surface temperature simulation for different land covers. J. Hydrol. 356, 327–343.

Hesslerová, P., Pokorný, J., 2010a. The synergy of solar radiation, plant biomass, and humidity as an indicator of ecological functions of the landscape: a case study from Central Europe. Integr. Environ. Assess. Manage. 6 (2), 249–259.

Hesslerová, P., Pokorný, J., 2010b. Forest clearing, water loss, and land surface rating as development costs. Int. J. Water 5 (4), 401–418.

Hesslerová, P., Chmelová, I., Pokorný, J., et al., 2012. Surface temperature and hydrochemistry as indicators of land cover functions. Ecol. Eng. 49, 146–152.

Huryna, H., Pokorný, J., 2010. Comparison of reflected solar radiation, air temperature and relative air humidity in different ecosystems. In: Vymazal, J. (Ed.), Water and Nutrient Management in Natural and Constructed Wetlands. Springer, New York, pp. 309–326.

IPCC, 2007. In: Pachauri RK, Reisinger A (Eds.), Climate Change—Synthesis Report. The Core Writing Team. http://www.ipcc.ch/ (accessed 28.03.10).

Jenerette, G.D., Harlan, S.L., Brazel, A., et al., 2007. Regional relationships between surface temperature, vegetation, and human settlement in a rapidly urbanizing ecosystem. Landscape Ecol. 22, 353–365.

Jim, C.Y., He, H., 2010. Coupling heat flux dynamics with meteorological conditions in the green roof ecosystem. Ecol. Eng. 36, 1052–1063.

Jirka, V., Hofreiter, M., Pokorný, J., Novák, M.,2009. Method for estimation of surface fluxes of solar energy in landscape based on remote sensing. In: VI-International Conference on Environmental Hydrology [CD-ROM]. American Society of Civil Engineers, Egypt, Cairo, pp. 1–13.

Jirka, V., Pokorný, J., Kobrzek, F. et al., 2011. Soustava prostředků pro zjišťování energetických toků v přízemní vrstvě atmosféry. Česká republika. Užitný vzor, 22671 U1. 2011-09-12. (The system for detecting energy flows in the ground layer of the atmosphere. The Czech Republic. Utility model, 22671 U1. 2011-09-12.).

Jiang, J., Tian, G., 2010. Analysis of the impact of land use/land cover change on land surface temperature with remote sensing. P. Environ. Sci. 2, 571–575.

Kadlec, R.H., 2009. The Houghton Lake wetland treatment project. Ecol. Eng. 35 (9), 1285–1286.

Kalnay, E., Cai, M., 2003. Impact of urbanization and land-use change on climate. Nature 423, 528–531.

Karnieli, A., Nurit, A., Pinker, R.T., et al., 2010. Use of NDVI and land surface temperature for drought assessment: merits and limitations. J. Clim. 23, 618–633.

Katsiabani, K., Adaktilou, N., Cartalis, C., 2009. A generalised methodology for estimating land surface temperature for non-urban areas of Greece through the combined use of NOAA–AVHRR data and ancillary information. Adv. Space Res. 43, 930–940.

Kędziora, A., 2010. Landscape management practices for maintenance and enhancement of ecosystem services in countryside. Ecol. Hydrobiol. 10 (2–4), 133–152.

Kravčík, M., Pokorný, J., Kohutiar, J., et al., 2007. Water for the Recovery of the Climate – A New Water Paradigm. Municipalia.

Květ, J., Jeník, J., Soukupová, L., 2002. Freshwater wetlands and their sustainable future: a case study of Třeboň basin biosphere reserve, UNESCO, Man and the Biosphere Series , Czech Republic, Paris.

Lambin, E.F., Ehrlich, D., 1996. The surface temperature-vegetation index space for land cover and land-cover change analysis. Int. J. Remote Sens. 17 (3), 63–487.

Lambin, E.F., Ehrlich, D., 1997. Land-cover changes in sub-Saharan Africa (1982–1991): application of a change index based on remotely sensed surface temperature and vegetation indices at a continental scale. Remote Sens. Environ. 61, 181–200.

Lawton, R.O., Nair, U.S., Pielke Sr., R.A., et al., 2001. Climatic impact of tropical lowland deforestation on nearby montane cloud forests. Science 294, 584–587.

Le-Xiang, Q., Hai-Shan, C., Jie, C., 2006. Impacts of land use and cover change on land surface temperature in the Zhujiang Delta. Pedosphere 16 (6), 681–689.

Leuzinger, S., Vogt, R., Körner, Ch., 2010. Tree surface temperature in an urban environment. Agric. Forest Meteorol. 150, 56–62.

Li, X., Ouyang, W., Xu, W., et al., 2012. Spatial pattern of greenspace affects land surface temperature: evidence from the heavily urbanized Beijing metropolitan area, China. Landscape Ecol., http://dx.doi.org/10.1007/s10980-012-9731-6.

Lillesand, T.M., Kiefer, R.W., 2000. Remote Sensing and Image Interpretation. John Wiley & Sons, Inc., New York.

Liski, J., Karjalainen, T., Pussine, A., et al., 2000. Trees as carbon sinks and sources in the European Union. Environ. Sci. Policy 3, 91–97.

Makarieva, A.M., Gorshkov, V.G., Li, B.-L., 2006. Conservation of water cycle on land via restoration of natural closed-canopy forests: implications for regional landscape planning. Ecol. Res. 21, 897–906.

Makarieva, A.M., Gorshkov, V.G., 2007. Biotic pump of atmospheric moisture as driver of the hydrological cycle on land. Hydrol. Earth Syst. Sci. 11 (2), 1013–1033.

Makarieva, A.M., Gorshkov, V.G., 2010. The biotic pump: condensation, atmospheric dynamics and climate. Int. J. Water 5 (4), 365–385.

McAlpine, C.A., Syktus, J., Ryan, J.G., et al., 2009. A continent under stress: interactions, feedbacks and risks associated with impact of modified land cover on Australia's climate. Glob. Change Biol. 15 (9), 2206–2223.

McPherson, R.A., 2007. A review of vegetation–atmosphere interactions and their influences on mesoscale phenomena. Prog. Phys. Geogr. 31, 261–285.

Melesse, A.M., 2004. Spatiotemporal dynamics of land surface parameters in the Red River of the North Basin. Phys. Chem. Earth 29, 795–881.

Mihailovic, D.T., Eitzinger, J., 2007. Modelling temperatures of crop environment. Ecol. Model. 202, 465–475.

Miko, L., Hošek, M., 2009. Příroda a krajina České republiky. Zpráva o stavu 2009. AOPK ČR, Praha (The Nature and the Landscape of the Czech Republic. A Report on the year 2009).

Moran, M.S., Peters-Lidard, C.D., Watts, J.M., et al., 1994. Estimating crop water deficit using the relation between surface-air temperature and spectral vegetation index. Remote Sens. Environ. 49, 246–263.

Nemani, R.R., Running, S.W., 1997. Land cover characterization using multitemporal red, near-IR, and thermal-IR data from NOAA/AVHRR. Ecol. Appl. 7 (1), 79–90.

Norman, J.M., Becker, F., 1995. Terminology in thermal infrared remote sensing of natural surfaces. Agric. Forest Meteorol. 77, 153–166.

Nuñez, M.N., Ciapessoni, H.H., Rolla, A., et al., 2008. Impact of land use and precipitation changes on surface temperature trends in Argentina. J. Geophys. Res. 113, D06111.

Pal Arya, S., 2001. Introduction to Micrometeorology. International Geophysics series, vol. 79. Academic Press, San Diego.

Penman, H.L., 1948. Natural evaporation from open water, bare soil and grass. Proc. R. Soc. A: Math. Phys. 193, 120–145.

Peters, R.T., Evett, S.R., 2007. Spatial and temporal analysis of crop conditions using multiple canopy temperature maps created with center-pivot-mounted infrared thermometers. Trans. ASABE 50 (3), 919–927.

Piao, S., Friedlingstein, P., Ciais, P., et al., 2007. Changes in climate and land use have a larger direct impact than rising CO_2 on global river runoff trends. Proc. Natl. Acad. Sci. U.S.A. 104 (39), 15242–15247.

Pielke Sr., R.A., 2001. Influence of the spatial distribution of vegetation and soils on the prediction of cumulus convective rainfall. Rev. Geophys. 39 (2), 151–177.

Pielke Sr., R.A., 2005. Land use and climate change. Science 310 (5754), 1625–1626.

Pielke, R.A., Beltrán-Przekurat, A., Hiemstra, C.A., et al., 2006. Impacts of regional land use and land cover on rainfall: an overview. In: Demuth, S., Gustard, A., Planos, E., et, al. (Eds.), Climate Variability and Change—Hydrological Impacts. IAHS Publ., pp. 325–332, 308.

Pokorný, J., 2001. Dissipation of solar energy in landscape – controlled by management of water and vegetation. Renew. Energy 24, 641–645.

Pokorný, J., Brom, J., Čermák, J., et al., 2010a. How water and vegetation control solar energy fluxes and landscape heat. Int. J. Water 5 (4), 311–336.

Pokorný, J., Květ, J., Rejšková, A., et al., 2010b. Wetlands as energy dissipating systems. J. Indus. Microbiol. Biotechnol. 37 (12), 1299–1305.

Procházka, J., Brom, J., Šťastný, J., et al., 2011. The impact of vegetation cover on temperature and humidity properties in the reclaimed area of a brown coal dump. Int. J. Mining, Reclam. Environ. 25, 350–366.

Quattrochi, D.A., Ridd, M.K., 1998. Analysis of vegetation within a semi-arid urban environment using high spatial resolution airborne thermal infrared remote sensing data. Atmos. Environ. 32 (1), 19–33.

Quattrochi, D.A., Luvall, J.C., 1999. Thermal infrared remote sensing for analysis of landscape ecological processes: methods and applications. Landscape Ecol. 14, 577–598.

Quattrochi, D.A., Luvall, J.C. (Eds.), 2004. Thermal Remote Sensing in Land Surface Processes. CRC Press, Florida.
Rejšková, A., Čížková, H., Brom, J., et al., 2012. Transpiration, evapotranspiration and energy fluxes in a temperate wetland dominated by *Phalaris arundinacea* under hot summer conditions. Ecohydrology 5 (1), 19–27.
Riecosky, D.C., Brown, P.W., Moran, M.S., 1994. Diurnal trends in wheat canopy temperature, photosynthesis, and evapotranspiration. Remote Sens. Environ. 49, 234–245.
Ripl, W., 2003. Water: the bloodstream of the biosphere. Philos. Trans. R. Soc. Lond. B 358, 1921–1934.
Ripl, W., 2010. Losing fertile matter to the sea: How landscape entropy affects climate. Int. J. Water 5 (4), 353–364.
Ripley, B.D., 1987. Stochastic Simulation. Wiley, New York.
Ryszkowski, L., Kędziora, A., 2008. The influence of plant cover structures on water fluxes in agricultural landscapes. In: Bossio, D., Geheb, K. (Eds.), Conserving Land, Protecting Water. CAB International/CABI, Wallingford, UK/Cambridge, MA, pp. 163–177.
Saunders, S.C., Chen, J., Crow, T.R., et al., 1998. Hierarchical relationships between landscape structure and temperature in a managed forest landscape. Landscape Ecol. 13, 381–395.
Shaver, G.R., Canadell, J., Chapin III, F.S., et al., 2000. Global warming and terrestrial ecosystems: a conceptual framework for analysis. Bioscience 50 (10), 871–882.
Strassburg, B., Turner, R.K., et al., 2009. Reducing emissions from deforestation—the "combined incentives" mechanism and empirical simulations. Global Environ. Change 19, 265–278.
Teemusk, A., Mander, Ü., 2010. Temperature regime of planted roofs compared with conventional roofing systems. Ecol. Eng. 36, 91–95.
Teuling, A.J., Seneviratne, S.I., Stöckli, M. et al., 2010. Contrasting response of European forest and grassland energy exchange to heatwaves. Nat. Geosci., http://dx.doi.org/10.1038/NGEO950. Advanced Online Publication www.nature.com/naturegeoscience
Trenberth, K.E., 2004. Rural land-use change and climate. Nature 427, 213.
Wanjura, D.F., Maas, S.J., Winslow, J.C., et al., 2004. Scanned and spot measured canopy temperatures of cotton and corn. Comput. Electron. Agric. 44, 33–48.
Xiao, H., Weng, Q., 2007. The impact of land use and land cover changes on land surface temperature in a karst area of China. J. Environ. Manage. 85, 245–257.
Yokohari, M., Brown, R.D., Kato, Y., et al., 1997. Effects of paddy fields on summertime air and surface temperatures in urban fringe areas of Tokyo, Japan. Landscape Urban Plan. 38, 1–11.